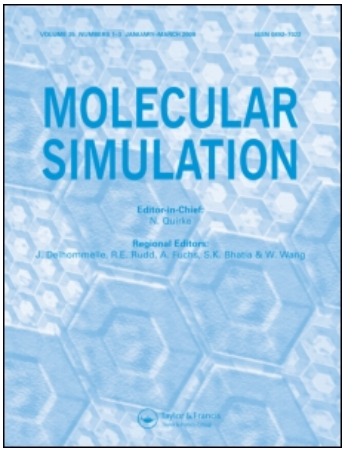

Molecular Simulation
Publication details, including instructions for authors and subscription information:
http://www.informaworld.com/smpp/title~content=t713644482

Spatial updating Monte Carlo algorithms in particle simulations

G. Orkoulas[a]
[a] Department of Chemical and Biomolecular Engineering, University of California, Los Angeles, CA, USA

Online publication date: 03 August 2010

To cite this Article Orkoulas, G.(2010) 'Spatial updating Monte Carlo algorithms in particle simulations', Molecular Simulation, 36: 7, 516 — 525
To link to this Article: DOI: 10.1080/08927022.2010.496785
URL: http://dx.doi.org/10.1080/08927022.2010.496785

Molecular Simulation
Vol. 36, Nos. 7–8, June–July 2010, 516–525

Taylor & Francis
Taylor & Francis Group

Spatial updating Monte Carlo algorithms in particle simulations

G. Orkoulas*

Department of Chemical and Biomolecular Engineering, University of California, Los Angeles, CA 90095, USA

(*Received 14 December 2009; final version received 7 February 2010*)

Spatial updating is a generalisation of random and sequential updating algorithms for Ising and lattice-gas systems to off-lattice, continuum fluid models. By analogy with a lattice-gas, spatial updating is implemented in the grand canonical ensemble by selecting a point in space and deducing the type of move by examining the local environment around the point. In this work, spatial updating is combined with simulated tempering techniques to determine the phase behaviour of a square-well fluid with an interaction range 1.15σ, where σ is the particle diameter. In the remaining part of this work, spatial updating is extended to very high densities by allowing volume fluctuations. In the resulting ensemble, a prototype of great grand canonical ensemble, fluctuations are unbounded and a constraint or a restriction must be imposed. Each simulation of the constrained great grand canonical ensemble requires a set of weights that are determined iteratively. The main outcome of a single simulation in the constrained great grand canonical ensemble is the density of states in terms of all its independent extensive variables, which allows for the determination of absolute free energies and entropies. Results obtained on a system of hard spheres demonstrate the validity of this technique.

Keywords: Monte Carlo; phase transitions; finite-size scaling

1. Introduction

Spatial updating Monte Carlo algorithms [1,2] are based on random and sequential updating algorithms [3–5] for Ising and lattice-gas systems. By analogy with the lattice-gas, the updating is realised in the grand canonical ensemble and is executed by selecting a point in space either at random or according to a prescribed order. The type of the elementary update (insertion or removal) is deduced by examining the local environment around the selected point. The motivation for the development of spatial updating algorithms is provided from recent analytical and numerical results for lattice systems suggesting that sequential updating algorithms yield samples of higher statistical quality than random updating algorithms [6]. Simulation results on square-well and Lennard-Jones fluids [1,2] indicate that spatial updating is more efficient than standard grand canonical updating [7,8] and is ideal for parallel implementation via domain decomposition.

Precise simulation of fluid–fluid and fluid–solid phase transitions, metastability and nucleation is a topic of considerable theoretical and practical importance. In protein and colloid crystallisation [9,10], it is believed that fluid–fluid demixing is metastable against solidification. Critical slowing down effects associated with the unbounded growth of correlations and fluctuations cause simulations to slow down substantially. Although significant progress has been achieved in devising collective updating techniques for lattice systems [11,12], there is no comparable grand canonical algorithm capable of attaining similar precision for continuum fluid models.

In a similar context, simulation of phase coexistence at low temperatures encounters difficulties due to tunnelling effects associated with the crossing of interfacial configurations that are intermediate to those of the two coexisting phases [13]. The previous problem may be alleviated by sampling from a suitably modified distribution that forces the highly improbable intermediate configurations to occur just as often as the configurations associated with the stable coexisting phases. These simulation techniques are commonly referred to as flat-histogram techniques, and they execute a nearly uniform random walk in terms of an order parameter [14–16] or a conjugate field variable [17–20].

In this work, the phase behaviour of a square-well model is investigated via spatial updating grand canonical Monte Carlo simulations. The interaction range is set to 1.15σ, where σ is the particle diameter. The simulations are combined with simulated tempering techniques [17,18] to enhance the infrequent transitions between the coexisting phases at low temperatures. In simulated tempering, several replicas of the system are coupled to form a super-ensemble or an expanded ensemble. Each of the different replicas corresponds to a grand canonical system at a given chemical potential and temperature. The elementary updates comprise particle transfers and transitions between different replicas. Particle transfers

*Email: makis@seas.ucla.edu

ISSN 0892-7022 print/ISSN 1029-0435 online

DOI: 10.1080/08927022.2010.496785
http://www.informaworld.com

are implemented according to the methodology of spatial updating. A heat-bath algorithm [21] is used for the replica switch step. The chemical potential μ and the temperature T of each replica are selected from the maximum compressibility line in the (μ,T) plane. The sequence of different replicas encompasses a range of states that correspond to both single- and two-phase systems. The vapour–liquid critical point is determined by finite-size scaling techniques using a fourth-order Landau expansion of the size-dependent free-energy density.

Previous works [22,23] on the square-well model with interaction range of 1.15σ indicate that vapour–liquid demixing is metastable against fluid–solid separation. Despite the fact that spatial updating allows the grand canonical sampling to explore very high densities, it cannot probe the solid phase. This happens because the solid is an expanded crystal in which the equilibrium distance between neighbouring lattice points is slightly greater than σ. The previous deficiency can be overcome by allowing for volume fluctuations in the grand canonical system. In so doing, one forms a so-called great grand canonical ensemble in which all intensive variables are fixed and all extensive variables fluctuate without bounds [24]. Since fluctuations are unbounded, Monte Carlo simulations in such a system cannot be implemented.

The remaining part of this work is associated with a successful implementation of spatial updating in the great grand canonical ensemble. To maintain fluctuations within bounds, a constraint or a restriction is imposed [24]. Each simulation in the constrained great grand canonical ensemble requires a set of weights that must be found via an iterative process. The main outcome of a single simulation is the density of states in terms of all its independent extensive variables which allows calculation of absolute free energies and entropies. The combination of spatial updating with volume expansions and contractions allows the simulation to explore very high densities. In this work, the method is applied to a system of hard spheres and its relative advantages and disadvantages are discussed.

2. Spatial updating grand canonical Monte Carlo

Consider a Monte Carlo simulation of an Ising model in an external magnetic field. In random updating [3–5], a site is selected at random with uniform probability and the orientation of the corresponding spin is reversed. In sequential updating [3–5], the sites are selected in a predetermined order. For example, for a square lattice, one may update the sites of the first row, then those of the second row, etc. For both cases, the updates are accepted with the same Metropolis acceptance criteria. The Ising model in an external magnetic field is equivalent to a grand canonical system of particles, the so-called lattice-gas [25], in which each site may be either empty or occupied by a particle. The updating is implemented by changing the identity of a site (i.e. occupied $\rightarrow$ empty or empty $\rightarrow$ occupied).

The properties of the transition matrices (kernels) associated with random and sequential updating for lattice systems have been investigated recently [6]. It has been proved analytically that the diagonal elements of the sequential sweep kernel are always smaller than those of the random sweep kernel [6]. The previous analytical result implies that sequential updating in Monte Carlo simulations may converge faster and yield samples of better statistical quality than random updating and can be understood by the following physical reasoning. For the Ising model, successful flip of spin triggers a higher probability of flipping a neighbouring spin. Likewise, for the lattice-gas, successful insertion (removal) of a particle at a site triggers a higher probability of successful insertion (removal) of a particle in a neighbouring site. Sequential updating takes advantage of this effect – the so-called neighbour effect [6] – and results in a 'cascaded' type of enhancement of sampling. In the case of random updating, these effects rarely occur due to the random selection of the site.

Now, consider the generalisation of random and sequential updating methods for lattice systems to continuum fluid models. In view of the equivalence of the Ising model to the lattice-gas, the development must be done in the grand canonical ensemble for which the elementary updates comprise particle insertions and removals. In contrast to standard grand canonical algorithms [7,8] and by analogy with the lattice-gas, the updating is implemented by selecting a point in space and deducing the update type by examining the local environment around that point. Hence, this type of updating has been dubbed *spatial updating* [1,2].

To this end, consider a grand canonical system of indistinguishable particles of diameter σ with no internal degrees of freedom, in a d-dimensional volume V at temperature T. The particles interact according to a pair-wise additive potential, e.g. Lennard-Jones. If μ is the chemical potential of the particles, the activity z of the particles is defined as $z = \Lambda^{-d}\exp(\beta\mu)$, where Λ is the thermal De Broglie wavelength, $\beta = 1/k_{\mathrm{B}}T$ and k_{B} the Boltzmann's constant. Consider a current configuration that contains N particles at positions $\mathbf{r}_1, \mathbf{r}_2, \ldots, \mathbf{r}_N$, as shown in Figure 1. In spatial updating [1,2], a uniform random point $\mathbf{r}$ is generated within the d-dimensional volume V. If $|\mathbf{r} - \mathbf{r}_n| > \sigma/2, \ \forall n = 1, 2, \ldots, N$, particle insertion is attempted and the position of the particle is obtained at random within a d-dimensional sphere of diameter σ: (see Figure 1). Particle removal is attempted when there is only one particle, m say (see also Figure 1), for which $|\mathbf{r} - \mathbf{r}_m| \leq \sigma/2$ and $|\mathbf{r} - \mathbf{r}_n| > \sigma/2 \ \forall n \neq m$. For these two cases, the Metropolis acceptance probability, α_{ij}, from state i that contains N particles to state j with $N \pm 1$ particles, is given by [1,2]:

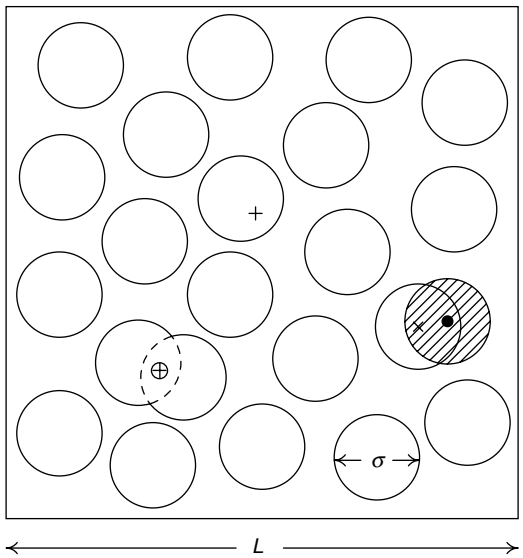

Figure 1. Two-dimensional illustration of the methodology of spatial updating (random updating). Points are generated randomly within the system volume (area), $V = L^2$. Point ' + ' corresponds to particle removal, whereas point ' × ' to particle insertion. In that case, the position of the particle, shown as '•' in the figure, is obtained at random within a sphere (circle) of diameter σ, centred at point ' × '. For points associated with double/multiple particle overlaps (such as '⊕' in the figure), the proposed update is rejected and the current state is counted again.

$$\alpha_{ij} = \min\{1, (zv)^{\pm 1} \exp(-\beta \Delta U)\}, \qquad (1)$$

where $(+)$ corresponds to insertion and $(-)$ to removal. In Equation (1), ΔU is the potential energy difference between states i and j and v the volume of a d-dimensional sphere of diameter σ. The case for which $|\mathbf{r} - \mathbf{r}_m| \leq \sigma/2$ for more than a single particle corresponds to double (or multiple) overlaps, see Figure 1. In such a case, the proposed update is rejected and the current state is counted again. Simulation results for two- and three-dimensional Lennard-Jones systems [2] indicate that the rejection of the update that corresponds to double/multiple overlaps does not affect sample quality.

A two-dimensional illustration of the sequential implementation of spatial updating is shown in Figure 2. Suppose that the length of the simulation box is $L = n\sigma$, where n is an integer. The d-dimensional volume $V = L^d$ is partitioned into n^d cells of side σ. These cells are labelled in a specific order, i.e. in terms of rows in the two-dimensional example shown in Figure 2. A uniform random point $\mathbf{r}$ is generated within a cell of side σ. Sequential updating corresponds to implementing the updating of Figure 1 in cell J in the order $J = 1, 2, \ldots, n^d$. After the completion of the n^d updates, another random point $\mathbf{r}$ is generated and the process is repeated. The elementary updates are accepted with the same Metropolis criteria as in the case of purely random updates, cf.

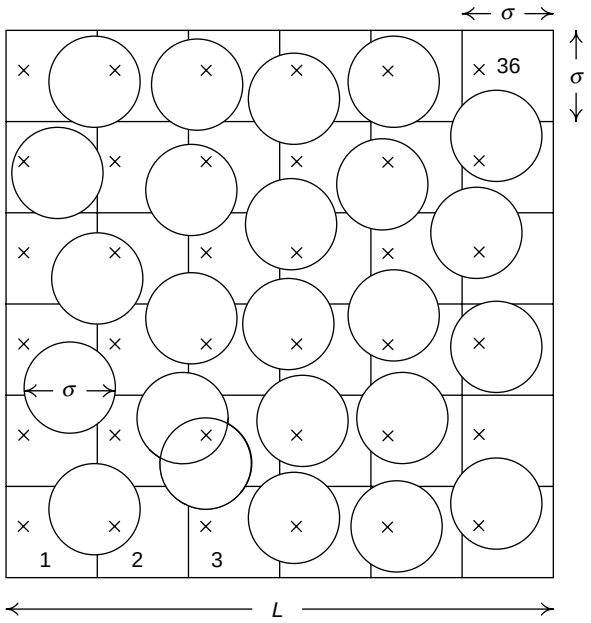

Figure 2. Two-dimensional illustration of the methodology of spatial updating (sequential updating). The length of the simulation box is $L = n\sigma$, where n is an integer. The simulation volume (area) $V = L^2$ is partitioned into n^2 cells of side σ. In the illustration, the n^2 cells are labelled in rows starting from the bottom left corner. A uniform random point $\mathbf{r}$ is generated within a cell of side σ. Sequential updating corresponds to implementing the updating of Figure 1 in cell J in the order $J = 1, 2, \ldots, n^2$. After the implementation of the n^2 updates, another random point $\mathbf{r}$ is generated within a cell of side σ and the process is repeated.

Equation (1). The division of the volume into d-dimensional cubes of side σ is one of many possibilities. In previous work on two-dimensional systems [26], the volume (area) was divided into n^2 hexagons of area $\sqrt{3}\sigma^2/2$ and side $\sqrt{3}\sigma/3$. For three-dimensional systems, the volume may be divided into $4n^3$ rhombic dodecahedra [24] [the Wigner–Seitz cell of the face-centred cubic (fcc) lattice] of volume $\sigma^3/\sqrt{2}$.

Previous works on square-well and Lennard-Jones systems [1,2] indicate that both the random and the sequential versions of spatial updating are more efficient than conventional updating. The superiority of random updating (cf. Figure 1) may be explained by the fact that the update type (insertion or removal) is deduced by the system based on the conditions around the selected point. In contrast, in conventional grand canonical updating, the update type is decided a priori with fixed probability. As in the case of lattice models [6], sequential updating (cf. Figure 2) is more efficient than random updating. Thus, successful insertion (removal) of a particle triggers a higher probability of another successful insertion (removal) of a particle in a neighbouring point in space. In addition, due to the nature of the updating, spatial updating grand canonical Monte Carlo is efficient at

densities that are much higher than possible with conventional grand canonical algorithms. More importantly, due to the nature of the updating, sequential updating for lattice and off-lattice continuum models is ideal for large-scale parallel implementation via geometric decomposition techniques [2,27]. In Section 3, the technique of spatial updating is used to determine the phase behaviour of a square-well fluid.

3. Simulation of phase transitions via spatial updating

Simulation studies of phase transitions are hampered by critical slowing down effects and by tunnelling effects associated with states of high free energy that are intermediate to those of the two coexisting phases [13]. Flat-histogram type of techniques [14–20] partially ameliorate these difficulties via a suitable modification of the sampling distribution. In this work, spatial updating grand canonical Monte Carlo is incorporated into simulated tempering techniques in order to deduce the phase behaviour of a square-well fluid. In simulated tempering [17,18], several replicas of the system are coupled to form a super-ensemble or an expanded ensemble. In the context of this work, each replica corresponds to a grand canonical system at temperature T_m (or inverse temperature β_m), chemical potential μ_m (or activity z_m) and volume V. If Ξ_m is the grand partition function of the m^{th} replica, the partition function Φ of the super-ensemble that consists of K replicas is defined as follows:

$$\Phi = \sum_{m=1}^{K} \Xi_m \mathrm{e}^{\eta_m}, \tag{2}$$

where η_m is a weighting factor associated with the m^{th} replica.

Inspection of the partition function in Equation (2) indicates that two types of Monte Carlo moves are possible: particle transfers and transitions between the K replicas. Particle transfers are implemented according to spatial updating (sequential implementation, see Figure 2) and accepted using Equation (1) with $z = z_m$ and $\beta = \beta_m$. The transitions between the K replicas are implemented according to a heat bath algorithm [21]. For a state of N particles with potential energy U, the transition probability, P_{mn}, from (T_m, μ_m) to (T_n, μ_n), is given by

$$P_{mn} = \frac{z_n^N \mathrm{e}^{-\beta_n U + \eta_n}}{\sum_{r=1}^{K} z_r^N \mathrm{e}^{-\beta_r U + \eta_r}}. \tag{3}$$

The weighting factors η_m control the frequency with which the K replicas appear during the simulation. From Equation (2), it follows that the probability, π_m, of observing the m^{th} replica is

$$\pi_m = \frac{1}{\Phi} \Xi_m \mathrm{e}^{\eta_m}. \tag{4}$$

The weighting factors η_m must be chosen such that π_m are nearly equal. If $F_m = \ln \Xi_m$ is the grand potential (free energy) at T_m and μ_m, the choice $\eta_m = -F_m$ renders $\pi_m = \text{const}$, i.e. each replica is visited with the same frequency. Since the free energies F_m are unknown, an iterative procedure is required during which the weights η_m are adjusted until the resulting distribution of π_m is nearly flat. An initial guess for the weights η_m is made, a short simulation is executed, the free energies F_m are estimated using histogram reweighting [28,29] and a refined estimate for η_m is obtained via $\eta_m = -F_m$. The previous process is repeated using the refined estimates for η_m at each iteration until the resulting histogram of π_m is nearly flat.

The square-well pair potential, $\phi(r)$, between two particles separated by distance r is defined as

$$\phi(r) = \begin{cases} \infty & r < \sigma, \\ -\epsilon & \sigma \le r \le \lambda\sigma, \\ 0 & r > \lambda\sigma. \end{cases} \tag{5}$$

In Equation (5), σ is the diameter of the particles, λ the range of the potential and $\epsilon > 0$ is the depth of the potential in units of energy. The value of $\lambda = 1.15$ is considered in this work. The model can be described by dimensionless parameters, the reduced temperature $T^* = k_{\mathrm{B}}T/\epsilon$ and the reduced activity $z^* = z\sigma^3$ or the reduced chemical potential $\tilde{\mu} = \ln(z^*)$. The dimensionless (reduced) density is $\rho^* = (N/V)\sigma^3 = \rho\sigma^3$, where N is the fluctuating number of particles and $\rho = N/V$ is the number density. In this work, the simulation volume, $V = L^3$, is partitioned into $4n^3$ rhombic dodecahedra of volume $\sigma^3/\sqrt{2}$ in which spatial updating as illustrated in Figure 2 is implemented. The linear extent of simulation box is $L = \sqrt{2}n\sigma$ with $n = 4, 5, \ldots, 10$.

In Monte Carlo studies of vapour–liquid phase transitions via a grand canonical type of updating, the simulations must cover both high-temperature, single-phase and low-temperature, two-phase states. Thus, a line is required that approximates the phase boundary in the μ-T plane and its extension in the single-phase region. For Ising and lattice-gas systems that are characterised by symmetry axes, the phase boundary and its single-phase extension coincide with the symmetry axis. Since no symmetry axes exist for continuum fluids, a line must be constructed that approximates the phase boundary and its extension in the high-temperature, single-phase region. In this work, the locus of inflection points of the density vs. chemical potential isotherms is chosen. This locus corresponds to the maximum of the susceptibility (or compressibility) defined as $\chi = (\partial\rho/\partial\mu)_T$. It should

be noted that the previous choice is not unique and other possibilities also exist, see [30] for example.

An estimate of the line of maximum susceptibility was established via Monte Carlo simulations of small systems (i.e. $n = 4$) using histogram reweighting [28,29]. A total of $K = 30-40$ replicas were considered on this line (depending on system size, L), encompassing both high-temperature single-phase and low-temperature two-phase states. For a given L, a single simulation that utilises spatial updating and tempering was implemented. An initial set of weights η_m was estimated from simulations of small system sizes. These weights were adjusted accordingly to render uniform sampling over the K replicas, as data for larger L became available. Once a suitable set of weights was determined, a long simulation of $50 - 200 \times 10^6$ sweeps (depending on system size), was executed. In this work, one sweep is defined as $4n^3$ elementary steps. The elementary updates comprise particle transfers and transitions between the K replicas. The frequency of transitions between the replicas was set to 0.25 sweeps and was implemented via a heat bath algorithm.

The vapour–liquid critical point (T_c, μ_c, ρ_c) may be obtained via finite-size scaling techniques [31,13]. According to finite-size scaling theory [31,13], a quantity F which exhibits a power-law type of divergence in the thermodynamic limit,

$$F \sim |t|^{-\omega} \quad \text{with } t = (T - T_c)/T_c, \tag{6}$$

scales asymptotically as

$$F(t, L) \approx L^{\omega/\nu} \tilde{F}(tL^{1/\nu}), \tag{7}$$

in the limit of large L. In Equation (7), ν is the exponent associated with the divergence of the correlation length and $\tilde{F}$ a universal scaling function. The scaling from of Equation (7) implies that F will reach an extremum (maximum or minimum) of height proportional to $L^{\omega/\nu}$. The location of the extremum, which may be regarded as an effective, L-dependent critical temperature $T_c(L)$, scales with L as

$$T_c(L) - T_c(\infty) \sim L^{-1/\nu}, \tag{8}$$

where $T_c(\infty)$ is the critical temperature in the limit of infinite system size. The critical parameters may thus be obtained by measuring second- and higher-order derivatives of the grand canonical free energy in terms of appropriate density-energy moments [30], locating the L-dependent peak positions and extrapolating in the limit of infinite size via Equation (8).

In this work, a simpler method, which is based on a Landau expansion of the L-dependent free energy density, $f_L(T, \rho)$, is used. The L-dependent critical parameters so obtained from $f_L(T, \rho)$ approach their respective infinite-size analogues from *above*, and the need to implement computationally expensive simulations at very low temperatures is thus avoided. The L-dependent free energy density, $f_L(T, \rho)$, is obtained from the grand canonical distribution of states using histogram reweighting [28,29]. For a finite system, f_L is analytic and it may thus be fitted to a Landau-type of expansion [26,30],

$$f_L(T, \rho) = \sum_{j=0}^{J} A_j(T; L)\rho^j, \tag{9}$$

where $J \geq 4$. The L-dependent critical point is found from $\partial^2 f_L/\partial\rho^2 = \partial^3 f_L/\partial\rho^3 = 0$, which corresponds to the vanishing of the inverse susceptibility.

The central portion ($0.27 \lesssim \rho^* \lesssim 0.60$) of f_L was fitted to the Landau form, Equation (9), with $J = 4$. The L-dependent values for the critical temperature $T_c(L)$ and chemical potential $\tilde{\mu}_c(L)$ were extrapolated towards $L \rightarrow \infty$ according to Equation (8), using $\nu = 0.630$ appropriate for systems in the three-dimensional Ising universality class [30]. The extrapolation of the effective critical parameters towards the limit of infinite size is shown in Figures 3 and 4. To minimise non-linearities associated with correction-to-scaling terms [32,33], the data that correspond to small systems ($n \leq 5$) were excluded from the fit. The data conform to a linear fit with satisfactory precision and yield $T_c^*(\infty) = 0.5754(3)$ and $\tilde{\mu}_c^*(\infty) = -2.6045 \pm 0.0015$. L-dependent values for the critical density were determined via histogram reweighting, using the previous estimates of the critical values of T and $\tilde{\mu}$. The best estimate for the critical density was taken

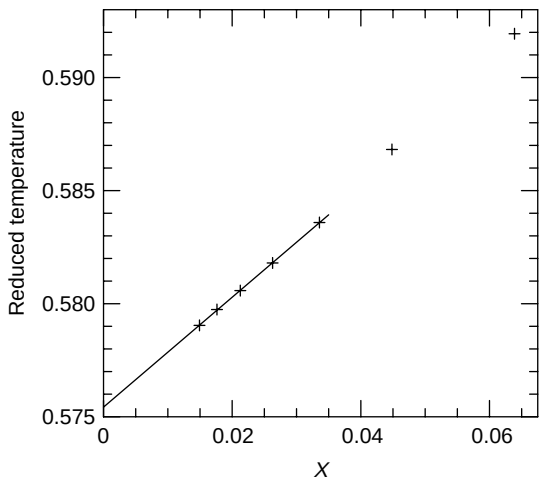

Figure 3. Critical temperature estimation for the square-well fluid with $\lambda = 1.15$. The L-dependent critical temperatures, $T_c^*(L)$, shown with crosses, (+), are obtained by analysing the Landau expansion of the canonical free energy density, f_L, cf. Equation (9). The effective critical temperatures are plotted vs. the scaling variable $X = (L/\sigma)^{-1/\nu}$, where $L = \sqrt{2}n\sigma$ and $\nu = 0.630$. The solid line is a linear fit. The data that correspond to $n = 4$ and 5 are excluded from the fit. The intersection of the solid line with the ordinate defines $T_c^*(\infty)$.

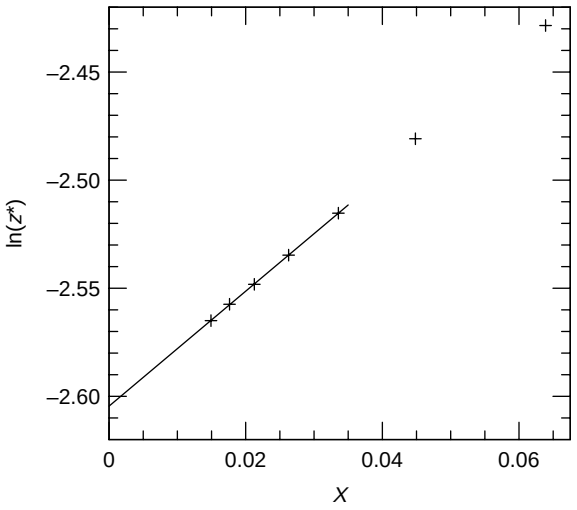

Figure 4. Estimation of the critical value of the chemical potential $\tilde{\mu} = \ln(z\sigma^3)$ for the square-well fluid with $\lambda = 1.15$. The procedure is analogous to that of Figure 3.

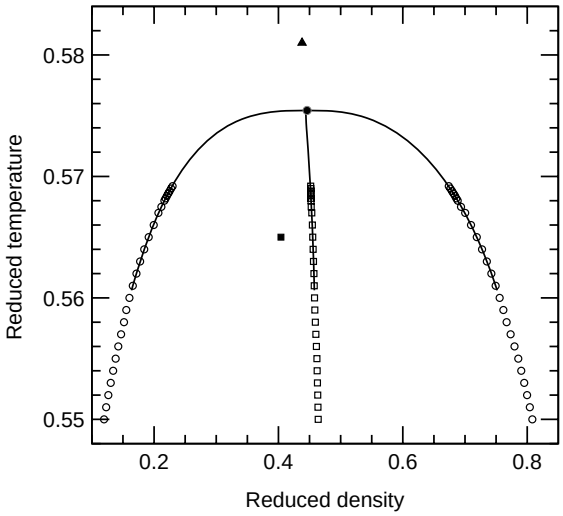

Figure 5. Vapour–liquid phase diagram for the square-well fluid with $\lambda = 1.15$ in the temperature–density plane. The open circles (◦) are estimates of the coexisting densities. The open squares (□) correspond to the coexistence curve diameter. The filled circle (•) is the critical point estimate obtained from a finite-size scaling analysis of the free energy density. The solid lines are fits to the Wegner forms, see Equations (10) and (11). The filled triangle and square are critical point estimates of previous work. (▲): Ref. [23]; (■): Ref. [22].

to be the average value of the L-dependent densities. Thus, $\rho_c^* = 0.446 \pm 0.001$ was the result of this calculation.

The critical point estimates obtained are plotted together with the estimates of the coexisting vapour and liquid densities in Figure 5. The coexisting densities have been determined by the so-called equal-weight criterion [34]. Since the simulated sizes correspond to small systems, the data do not extend sufficiently close to the critical point. In Figure 5, the coexistence data are fitted to Wegner-type of expansions [30]. Specifically, if $\rho^*_{\rm vap}(T)$ and $\rho^*_{\rm liq}(T)$ are the coexisting densities, the width of the coexistence curve may be expressed as:

$$\rho^*_{\rm liq}(T) - \rho^*_{\rm vap}(T) \simeq B|t|^{\beta}\Big[1 + b_\theta|t|^{\theta} + b_{2\beta}|t|^{2\beta}\Big], \quad (10)$$

where $t = (T - T_c)/T_c$. The three-dimensional Ising values have been adopted for the exponents in Equation (10). Thus, $\beta = 0.326$, $\alpha = 0.109$ and $\theta = 0.52$ [35]. The coexistence curve diameter, $\rho^*_{\rm diam}(T) = (1/2)\times[\rho^*_{\rm liq}(T) + \rho^*_{\rm vap}(T)]$, may likewise be fitted to the following Wegner form [30]:

$$\rho^*_{\rm diam}(T) \simeq \rho_c^* + a_{2\beta}|t|^{2\beta} + a_{1-\alpha}|t|^{1-\alpha} + a_1 t. \quad (11)$$

The critical point estimate of this work seems to be in disagreement with previous estimates [22,23], see Figure 5. A likely explanation for this difference may be the absence of the finite-size scaling analysis of the simulation data in those studies.

The combination of spatial updating grand canonical Monte Carlo with tempering techniques and finite-size scaling theory results in accurate determination of fluid–fluid phase diagrams. In a slightly different context, the determination of phase diagrams associated with very dense, nearly incompressible phases is an issue of considerable theoretical and practical importance. In protein and colloid crystallisation, for instance, it is believed that fluid–fluid demixing is metastable [9,10]. In the context of the square-well model, previous work indicates that for $\lambda = 1.15$, vapour–liquid separation is metastable against fluid–solid demixing [22,23]. Despite the fact that spatial updating is capable of sampling very high densities, it can never probe a solid phase. The equilibrium solid phase is an expanded crystal in which the equilibrium distance between neighbouring lattice points is slightly greater than the particle diameter σ. In the simulations described here, the volume was divided into $4n^3$ rhombic dodecahedra for which the distance between neighbours is exactly σ. Since the volume is fixed, a stable solid phase can never be seen. It may be argued that an increase in the distance between the cells might offer a better chance of sampling the solid phase. Such a task, however, is impractical since it is tantamount to implement *all* the simulations for different values of the nearest neighbour distance. A more efficient way, which is described in Section 4, is to allow for volume fluctuations in a grand canonical system.

4. Spatial updating in the great grand canonical ensemble

Consider a grand canonical system of particles for which the volume is also allowed to fluctuate. Such a case

corresponds to the so-called great grand canonical ensemble [36,37], with partition, Z, defined as follows:

$$Z = \sum_{N,V,E} W(N,V,E)\exp(-\beta E - \beta pV + \beta\mu N), \quad (12)$$

where p is the pressure, E the energy and $W(N,V,E)$ the degeneracy or the density of states or the microcanonical partition function [38]. Using the well-known connection of W with entropy S, $W = \exp(S/k_B)$ and the thermodynamic identity $E = TS - pV + \mu N$, it can be trivially shown that $Z \equiv 1$ which implies that the corresponding thermodynamic potential is zero. Since the intensive variables, μ, p and T, in Equation (12) are fixed, and the fluctuations of the extensive variables, N, V and E, are unbounded. Thus, simulations of a system with partition function given by Equation (12) cannot be implemented.

Suppose that a constraint or a restriction is imposed on the previous system to keep the fluctuations with certain bounds. For example, upper and lower bounds may be imposed on the extensive variables, e.g. $N_{\min} \le N \le N_{\max}$ and/or $V_{\min} \le V \le V_{\max}$ and/or $E_{\min} \le E \le E_{\max}$. It is important to emphasise that the selection of the constraint is not unique and other choices also exist. The resulting system then corresponds to a restricted or a constrained great grand canonical ensemble.

The next step in the construction of a Monte Carlo method associated with a constrained great grand canonical ensemble is the specification of the intensive variables. Note that only two of the three intensive variables μ, p and T can be specified independently. Consider the case for which p and T are specified and suppose that a constraint is imposed on N, i.e. $N_{\min} \le N \le N_{\max}$. The partition function associated with N particles at p and T, $\Delta(N,p,T)$, is defined as:

$$\Delta(N,p,T) = \sum_V Q(N,V,T)\,\mathrm{e}^{-\beta pV}, \quad \text{where} \quad (13)$$

$$Q(N,V,T) = \sum_E W(N,V,E)\,\mathrm{e}^{-\beta E} \quad (14)$$

is the canonical partition function of a system of N particles at V and T. The constrained great grand canonical ensemble can be obtained by coupling these isobaric systems via a Boltzmann type of factor. By analogy with the construction of the expanded ensemble in simulated tempering [17,18] techniques [cf. Equation (2)], the isobaric systems are connected with a weighting factor of the form $\exp(\beta G_N)$ to yield a constrained great grand canonical ensemble with partition function, Z^*, defined as:

$$Z^* = \sum_N^* \Delta(N,p,T)\,\mathrm{e}^{\beta G_N}. \quad (15)$$

The set of N-dependent weights G_N plays the same role as η_m in Equation (2) and '$*$' signifies the presence of a constraint. If μ_N is the value of the chemical potential of a system of N particles at p and T, the assignment

$$\beta G_N = \beta\mu_N N = -\ln\Delta(N,p,T), \quad (16)$$

i.e. the Gibbs function for N particles at p and T will result in uniform sampling of all N within $[N_{\min}, N_{\max}]$. The previous construction is not unique. Alternatively, one may construct the restricted great grand canonical ensemble as an expanded ensemble of grand canonical systems at the same chemical potential μ and temperature T but at different volumes, see [24] for example.

Inspection of Equation (15) indicates that three types of Monte Carlo moves are possible: particle displacements, volume changes and particle transfers. Displacements and volume changes are accepted with ordinary Metropolis type of criteria [21]. In this work, the particle transfer step is implemented according to the methodology of spatial updating. The acceptance probability is given by:

$$\alpha_{ij}^{(\pm)} = \min\{1, v^{\pm 1}\exp(\beta\Delta G - \beta\Delta E)\}, \quad (17)$$

where $(+)$ corresponds to insertion and $(-)$ to removal. In Equation (17), ΔE is the energy difference between state i with N particles and state j with $N \pm 1$ particles, $\Delta G = G_{N\pm1} - G_N$ and v the volume of a d-dimensional sphere. Transitions that violate the constraint $N_{\min} \le N \le N_{\max}$ are rejected and the current state is counted again. Thus, the system never escapes the window $N_{\min} \le N \le N_{\max}$. Each simulation requires specification of the temperature T, pressure p, constraint $N_{\min} \le N \le N_{\max}$ and set of weights or free energies G_N. The outcome of the simulation is the joint probability of N, V and E, $\mathcal{P}(N,V,E)$, defined as

$$\mathcal{P}(N,V,E) \propto W(N,V,E)\,\mathrm{e}^{\beta G_N - \beta pV - \beta E}, \quad (18)$$

and obtained as a histogram of observations in the course of the simulation. If $\beta G_N = -\ln\Delta$, it follows from Equation (7) that $\mathcal{P}(N,V,E) = $ const. within the (N,V,E) range allowed by the constraint. Since a simulation is of finite length, $\mathcal{P}(N,V,E)$ cannot be normalised. Thus, the measurement of $\mathcal{P}(N,V,E)$ as a histogram yields the density of states, $W(N,V,E)$, up to a proportionality constant, in terms of all its independent variables. As in previous flat-histogram techniques, a suitable set of free energies G_N must be found iteratively. The determination of the set of G_N is analogous to that of η_m [cf. Equation (4)]. Once satisfactory estimates for G_N have been found, a long simulation is executed to collect good quality statistics and obtain $W(N,V,E)$.

Once $W(N,V,E)$ has been determined, various averages such as microcanonical, canonical, grand canonical and isobaric can be calculated using histogram reweighting [28,29], see also Ref. [24]. In addition, since all extensive variables, N, V and E, vary (i.e. fluctuate), the variation of the partition functions with respect to those variables can

be calculated, which allows for the determination of absolute free energies and entropies. For example, for N particles at V and T, the pressure and the chemical potential may be found from [38]

$$\beta p = (\partial \ln Q/\partial V)_{N,T}, \quad \beta\mu = -(\partial \ln Q/\partial N)_{V,T}, \quad (19)$$

by approximating the derivatives with finite difference equations. Likewise, the chemical potential of N particles at p and T is found from [38]

$$\beta\mu = -(\partial \ln \Delta/\partial N)_{p,T}. \quad (20)$$

The main advantage of this type of simulation is the determination of the density of states, $W(N,V,E)$, in terms of all its independent extensive variables which allows for the calculation of absolute free energies and entropies. The simulation technique described here executes a nearly uniform random walk in N, V and E. In most previous flat-histogram techniques [14–18], one (or more) of the variables (N,V,E) are fixed, and thus only free energy differences can be calculated. In addition, the combination of spatial updating with volume dilations and contractions allows the simulation to explore very high densities and results in enhanced statistical performance. The main factor that determines the length of each simulation is the number of entries in the histogram of N, V and E, $\mathcal{P}(N,V,E)$. Each (N,V,E) entry must be visited a sufficient number of times to yield a precise determination of $W(N,V,E)$ and a consistent calculation of the required derivatives of W without spurious noise.

The previous method was used to determine the entropy of $N = 256$ hard spheres from simulations of a constrained great grand canonical ensemble with $200 \leq N \leq 300$. The details of these simulations can be found elsewhere [24]. Starting from the thermodynamic identity $E = TS - pV + \mu N$, it can be shown that the entropy relative to that of an ideal gas at the same thermodynamic state is given by:

$$\frac{\Delta S}{Nk_B} = \frac{\beta U}{N} + \left(\frac{\beta p}{\rho} - 1\right) - \ln\left(\frac{z}{\rho}\right), \quad (21)$$

where U is the potential energy, ρ the density and z the activity. Note that $U \equiv 0$ for hard spheres. The ideal gas entropy, S_0, is of the form [38] $S_0/Nk_B = -\ln(\rho^*) + f(T)$, where the T-dependent term contains quantum mechanical constants (i.e. Planck's constant). The results for 256 hard spheres, shown in Figure 6, are in very good agreement with the prediction of the Carnahan and Starling equation [39]. The circles correspond to 256 hard spheres at constant pressure. The density required in Equation (21) was obtained by histogram reweighting [28,29]. The corresponding value of μ (activity) was found by approximating the derivative in Equation (20) with a centred finite difference equation. Other types of approximations gave nearly identical results. The crosses in Figure 6 correspond to 256 hard spheres at constant volume. In that case, μ and p were estimated from Equation (19).

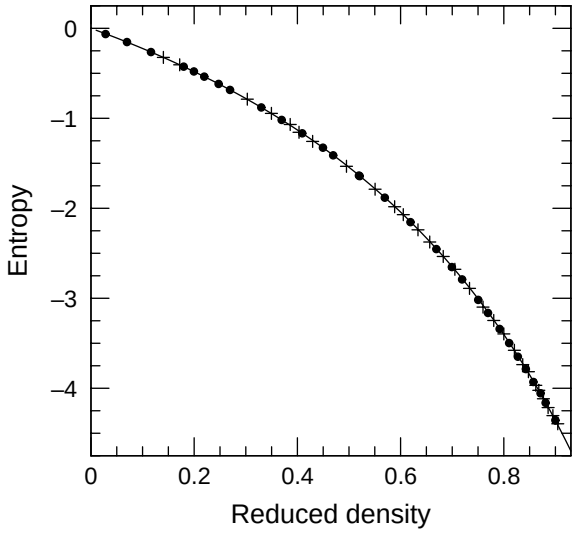

Figure 6. Entropy, $\Delta S/Nk_B$, relative to that of an ideal gas at the same thermodynamic state vs. reduced density, $\rho^* = \rho\sigma^3$, for the hard sphere fluid obtained from great grand canonical Monte Carlo simulations. The filled circles (•) correspond to $N = 256$ particles at constant pressure. The crosses (+) correspond to $N = 256$ particles at constant volume. The solid line is the Carnahan and Starling [39] result. Statistical errors do not exceed the symbol sizes.

For reduced densities $\rho^* = \rho\sigma^3 \gtrsim 0.94$, the hard sphere fluid undergoes a first-order phase transition to a fcc crystal [40,41]. In the previous work [24], it was shown that it is possible to locate this transition via simulations in a constrained great grand canonical ensemble. Since there is no terminal (i.e. critical) point for fluid–solid transitions, it is difficult to implement a procedure analogous to that used in the determination of the fluid-phase diagram of the square-well fluid. In Ref. [24], the fluid and the solid phases of the hard sphere model were simulated independently via constrained great grand canonical simulations. A modification of the cell model of Hoover and Ree [40,41] was used to simulate the fcc crystal and the relation $\mu = \mu(p)$ was established for both phases. The point at which these two $\mu - p$ curves intersect defines fluid–solid coexistence. Regarding transitions involving solid phases, the lattice or phase switch Monte Carlo method of Wilding and Bruce [42], which utilises a constant pressure ensemble, is currently the only method that leads to direct determination of phase equilibria of this type. In future work, spatial updating in the great grand canonical ensemble will be combined with phase/lattice switch updating to lead to direct determination of phase equilibria involving solid phases.

5. Discussion and conclusions

Spatial updating Monte Carlo algorithms are generalisations of random and sequential updating algorithms for lattice-gas type of systems to continuum fluid models. They work in 'open' ensembles for which the number of particles is not conserved. They cannot be applied to canonical Monte Carlo simulations since the density is constant. In fact, due to particle indistinguishability, random and sequential updating of *particles* in canonical Monte Carlo simulations are identical [43]. The key difference between spatial and conventional grand canonical updating is the way by which the elementary steps are implemented. Rather than a priori deciding on the move type (insertion or removal), the update type is deduced based on the local conditions of a point in space. If the sequence of points is selected appropriately (cf. Figure 2), correlations that develop in space between particles can be reduced and enhancement may be obtained.

Spatial updating algorithms are ideal for simulations of phase transitions, since they work in open ensembles for which the number of particles is not conserved and both the energy and the density fluctuate. However, in order to overcome the infrequent transitions between the coexisting phases they must be combined with flat-histogram techniques. In this work, the fluid-phase behaviour of a short-range square-well model was investigated via a combination of spatial updating grand canonical Monte Carlo simulations and simulated tempering techniques. The relative merits of the combination of grand canonical spatial updating with tempering techniques compared to conventional simulations have been described in the previous work [26]. The statistical and computational (i.e. total simulation time) performance depends on the number of replicas, their spacing and the frequency of transitions between different replicas. In the investigation of two-dimensional criticality, it was found [26] that the efficiency enhancement is 2–4 orders of magnitude higher than conventional algorithms. The simulation data for the square-well fluid were analysed via finite-size scaling techniques and the vapour–liquid-phase diagram and the concomitant critical point were obtained with high precision. Despite the fact that grand canonical spatial updating is efficient at very high densities, it cannot probe the solid phase and thus cannot be used to simulate fluid–solid transitions. Another drawback is associated with the amount of data required to perform a reliable finite-size scaling analysis. In these studies, one obtains L-dependent values for the critical parameters for a series of progressively increasing values of L and extrapolates towards the $L \rightarrow \infty$ limit. For each different values of L, an independent simulation must be employed (see, for instance, Figures 3 and 4) which is, clearly, a computationally time-consuming task. It would be more efficient, if one could gather the data in Figures 3 and 4 from a *single* simulation.

A solution to the previous drawbacks can be achieved by incorporating volume fluctuations in a grand canonical system. Such a set-up corresponds to a great grand canonical ensemble for which all intensive variables are fixed and all extensive variables fluctuate without bounds. To bound the range of fluctuations, a constraint or a restriction must be placed on the system. The resulting constrained great grand canonical ensemble can be constructed as a superposition of either constant-pressure or grand canonical systems that are coupled together via weighting functions. These weights must be found via an iterative process. A single simulation in the constrained great grand canonical ensemble comprises a nearly uniform random walk in terms of all the extensive variables within the range permitted by the constraint. Thus, this method belongs to the general class of flat-histogram techniques. The main outcome of a single simulation in this ensemble is the density of states in terms of all its independent extensive variables, which allows for calculation of free energies and entropies.

Incorporation of spatial updating in a constrained great grand canonical ensemble allows the simulations to explore very high densities and can lead to determination of fluid–solid equilibria. So far, this method has only been applied to a system of hard spheres. The major advantage of this technique is the determination of the density of states in terms of all its independent variables. The two main drawbacks are associated with the length of the simulations and the computational requirements of the volume change moves. The primary factor that determines the length of the simulations is the number of entries in the histogram of $\mathcal{P}(N,V,E)$, see Equation (18). Each entry must be visited a sufficient number of times so that a reliable estimate of the density of states can be obtained. The computational requirements of the volume change move depend strongly on the details of the intermolecular pair potential. These problems are also encountered in constant-pressure simulations. For simple cases, the energy change associated with a volume update can be obtained via rescaling. For most cases, however, a complete energy calculation is required, which is an order of N^2 computation. In this respect, the feasibility of parallel processing is crucial for the success of this method.

Acknowledgements

Financial support from NSF, CBET-0652131 and CBET-0967291 is gratefully acknowledged.

References

[1] G. Orkoulas, *Acceleration of Monte Carlo simulations through spatial updating in the grand canonical ensemble*, J. Chem. Phys. 127 (2007), pp. 084106-1–084106-9.

[2] C.J. O'Keeffe, R. Ren, and G. Orkoulas, *Spatial updating grand canonical Monte Carlo algorithms for fluid simulation: Generalization to continuous potentials and parallel implementation*, J. Chem. Phys. 127 (2007), pp. 194103-1–194103-8.
[3] L.D. Fosdick, *Calculation of order parameters in a binary alloy by the Monte Carlo Method*, Phys. Rev. 116 (1959), pp. 565–573.
[4] J.R. Ehrman, L.D. Fosdick, and D.C. Handscomb, *Computation of order parameters in an Ising lattice by the Monte Carlo method*, J. Math. Phys. 1 (1960), pp. 547–558.
[5] D.A. Chesnut and Z.W. Salsburg, *Monte Carlo procedure for statistical mechanical calculations in a grand canonical ensemble of lattice systems*, J. Chem. Phys. 38 (1963), pp. 2861–2875.
[6] R. Ren and G. Orkoulas, *Acceleration of Markov chain Monte Carlo simulations through sequential updating*, J. Chem. Phys. 124 (2006), pp. 064109-1–064109-8.
[7] G.E. Norman and V.S. Filinov, *Investigations of phase transitions by a Monte Carlo Method*, High Temp. (USSR) 7 (1969), pp. 216–222.
[8] D.J. Adams, *Grand canonical ensemble Monte Carlo for a Lennard-Jones fluid*, Mol. Phys. 29 (1975), pp. 307–311.
[9] D. Frenkel, *Entropy-driven phase transitions*, Phys. A 263 (1999), pp. 26–38.
[10] M.G. Noro, N. Kern, and D. Frenkel, *The role of long-range forces in the phase behavior of colloids and proteins*, Europhys. Lett. 48 (1999), pp. 332–338.
[11] R.H. Swendsen and J.-S. Wang, *Nonuniversal critical dynamics in Monte Carlo simulations*, Phys. Rev. Lett. 58 (1987), pp. 86–88.
[12] U. Wolff, *Collective Monte Carlo updating for spin systems*, Phys. Rev. Lett. 62 (1989), pp. 361–364.
[13] K. Binder, *Applications of Monte Carlo methods to statistical physics*, Rep. Prog. Phys. 60 (1997), pp. 487–559.
[14] B.A. Berg and T. Neuhaus, *Multicanonical ensemble: A new approach to simulate first-order phase transitions*, Phys. Rev. Lett. 68 (1992), pp. 9–12.
[15] J. Lee, *New Monte Carlo algorithm: Entropic sampling*, Phys. Rev. Lett. 71 (1993), pp. 211–214.
[16] F. Wang and D.P. Landau, *Efficient multiple-range random walk to calculate the density of states*, Phys. Rev. Lett. 86 (2001), pp. 2050–2053.
[17] E. Marinari and G. Parisi, *Simulated tempering: A new Monte Carlo scheme*, Europhys. Lett. 19 (1992), pp. 451–458.
[18] A.P. Lyubartsev, A.A. Martinovski, S.V. Shevkunov, and P.N. Vorontsov-Velyaminov, *New approach to Monte Carlo calculation of the free energy: Method of expanded ensembles*, J. Chem. Phys. 96 (1992), pp. 1776–1783.
[19] R.H. Swendsen and J.-S. Wang, *Replica Monte Carlo simulation of spin glasses*, Phys. Rev. Lett. 75 (1986), pp. 2607–2609.
[20] K. Hukushima and K. Nemoto, *Exchange Monte Carlo method and application ot spin glass simulations*, J. Phys. Soc. Jpn 65 (1996), pp. 1604–1608.
[21] D.P. Landau and K. Binder, *A Guide to Monte Carlo Simulations in Statistical Physics*, Cambridge University Press, Cambridge, 2000.
[22] D.L. Pagan and J.D. Gunton, *Phase behavior of short-range square-well model*, J. Chem. Phys. 122 (2005), pp. 184515-1–184515-6.
[23] H. Liu, S. Garde, and S. Kumar, *Direct determination of phase behavior of square-well fluids*, J. Chem. Phys. 123 (2005), pp. 174505-1–174505-4.
[24] G. Orkoulas and D.P. Noon, *Spatial updating in the great grand canonical ensemble*, J. Chem. Phys. 131 (2009), pp. 161106-1–161106-4.
[25] K. Huang, *Statistical Mechanics*, Wiley, New York, 1963.
[26] D.P. Noon and G. Orkoulas, *Simulations of phase transitions via spatial updating and tempering*, Mol. Simul 36 (2010), pp. 534–554.
[27] R. Ren and G. Orkoulas, *Parallel Markov chain Monte Carlo simulations*, J. Chem. Phys. 126 (2007), pp. 211102-1–211102-4.
[28] A.M. Ferrenberg and R.H. Swendsen, *New Monte Carlo technique for studying phase transitions*, Phys. Rev. Lett. 61 (1988), pp. 2635–2638.
[29] A.M. Ferrenberg and R.H. Swendsen, *Optimized Monte Carlo data analysis*, Phys. Rev. Lett. 63 (1989), pp. 1195–1198.
[30] G. Orkoulas, M.E. Fisher, and A.Z. Panagiotopoulos, *Precise simulation of criticality in asymmetric fluids*, Phys. Rev. E 63 (2001), pp. 051507-1–051507-14.
[31] M.E. Fisher and M.N. Barber, *Scaling theory for finite-size effects in the critical region*, Phys. Rev. Lett. 28 (1972), pp. 1516–1519.
[32] M.E. Fisher, *The renormalization group in the theory of critical behavior*, Rev. Mod. Phys. 46 (1974), pp. 597–616.
[33] Y.C. Kim and M.E. Fisher, *Asymmetric fluid criticality. II. Finite-size scaling for simulations*, Phys. Rev. E 68 (2003), pp. 041506-1–041506-23.
[34] C. Borgs and R. Kotecky, *Finite-size effects at asymmetric first-order phase transitions*, Phys. Rev. Lett. 68 (1992), pp. 1734–1737.
[35] R. Guida and J. Zinn-Justin, *Critical exponents of the N-vector model*, J. Phys. A 31 (1998), pp. 8103–8121.
[36] E.A. Guggenheim, *Thermodynamics*, 2nd ed., North Holland, Amsterdam, 1950.
[37] R.A. Sack, *Pressure-dependent partition functions*, Mol. Phys. 2 (1959), pp. 8–22.
[38] D.A. McQuarrie, *Statistical Mechanics*, University Science, Sausalito, 2000.
[39] N.F. Carnahan and K.E. Starling, *Equation of state for nonattracting rigid spheres*, J. Chem. Phys. 51 (1969), pp. 635–636.
[40] W.G. Hoover and F.H. Ree, *Use of computer experiments to locate the melting transition and calculate the entropy in the solid phase*, J. Chem. Phys. 47 (1967), pp. 4873–4878.
[41] W.G. Hoover and F.H. Ree, *Melting transition and communal entropy for hard spheres*, J. Chem. Phys. 49 (1968), pp. 3609–3617.
[42] N.B. Wilding and A.D. Bruce, *Freezing by Monte Carlo phase switch*, Phys. Rev. Lett. 85 (2000), pp. 5138–5141.
[43] C.J. O'Keeffe and G. Orkoulas, *Parallel canonical Monte Carlo simulations through sequential updating of particles*, J. Chem. Phys. 130 (2009), pp. 134109-1–134109-6.